

## Solid-State 2D-Heteronuclear $^{27}\text{Al}$ - $^{31}\text{P}$ Correlation NMR Spectroscopy of Aluminophosphate VPI-5

Ernst R. H. van Eck\* and Wiebren S. Veeman†

N.S.R. Center for Molecular Design  
Synthesis and Structure  
Laboratory of Molecular Spectroscopy  
University of Nijmegen  
Toernooiveld, 6525 ED Nijmegen, The Netherlands

Received June 22, 1992

A new 2D-heteronuclear correlation pulse sequence for solids under MAS has been developed, which enables the correlation of spectra of two different nuclei through their weak heteronuclear dipolar coupling. The sequence provides an alternative to other 2D-correlation techniques<sup>1,2</sup> for establishing through-space correlations, and employs a coherence transfer pulse sequence somewhat similar to the TEDOR experiment.<sup>3</sup>

Figure 1 displays the rotor-synchronized pulse sequence. The preparation period is a REDOR pulse sequence<sup>4</sup> which (partly) transfers  $I_y$  magnetization into  $2I_xS_z$  antiphase coherence. During the evolution period, the  $2I_xS_z$  coherence evolves under the Hamiltonian  $\mathcal{H}(t)$  for a time  $t_1$ :

$$\mathcal{H}(t) = \omega_I I_z + \omega_I(t) I_z + \omega_S S_z + \omega_S(t) S_z + \omega_D(t) 2I_x S_z$$

where the time-dependent terms are due to the effect of spinning on the chemical shift ( $\omega_I(t)$ ,  $\omega_S(t)$ ) and the dipolar coupling ( $\omega_D(t)$ ). The remaining antiphase magnetization is then stored as  $\pm 2I_x S_z$  coherence and converted into  $\pm 2I_x S_y$  antiphase magnetization at the completion of a rotor period. A second REDOR pulse sequence then produces observable  $S$ -spin magnetization,  $\pm S_x$ . The  $S$ -spin FID is now modulated with the intensity of the  $I$ -spin FID at  $t = t_1$ .

This pulse sequence was applied to the hydrated form of aluminophosphate molecular sieve VPI-5.<sup>5</sup> VPI-5 contains 18-membered rings, made from 6-membered and 4-membered rings. The framework symmetry of hydrated VPI-5 (space group  $P6_3$ )<sup>6</sup> gives rise to three different crystallographic sites (Figure 2). Al1 is octahedrally coordinated to four oxygens and two water molecules, whereas Al2 and Al3 are tetrahedrally coordinated to four oxygens. The  $^{27}\text{Al}$  NMR spectrum shows two lines with an intensity ratio of 2:1 for, respectively, the tetrahedral peak at 40 ppm and the octahedral peak, Al1, at -15 ppm. The  $^{27}\text{Al}$  DOR spectrum<sup>7</sup> reveals that the tetrahedral peak consists of two lines with an intensity ratio of 1:1. Grobet et al.<sup>8</sup> assigned the tetrahedral peak at 30.6 ppm (4.7 T) to Al2 since this peak is much more affected by the second-order quadrupole effect than the peak at 40.5 ppm (Al3). Engelhardt,<sup>9</sup> however, concluded that this assignment should be interchanged. The  $^{31}\text{P}$  spectrum shows three lines of equal intensity, at -23.7, -27.5, and at -33.2 ppm. Various authors have assigned the phosphorus peak at -33.2 ppm to the P1 site,<sup>10-14</sup> while Derouane et al.<sup>15,16</sup> assigned the peak at -23.7

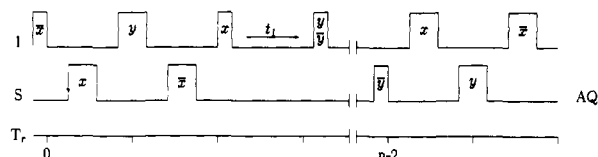


Figure 1. Pulse scheme used in the 2D-correlation experiment. The narrow blocks represent 90-deg pulses, the wide ones 180-deg pulses.

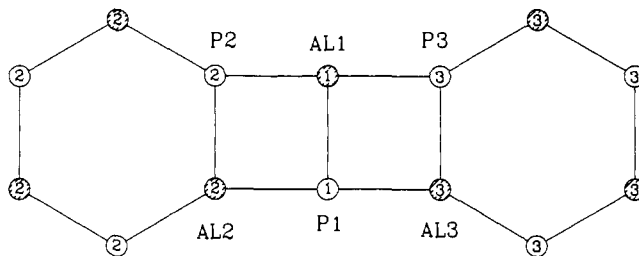


Figure 2. Schematic drawing of a part of the VPI-5 structure. The phosphorus atoms are represented by open circles, the aluminum by hatched circles. The oxygen atoms are not shown here for clarity.

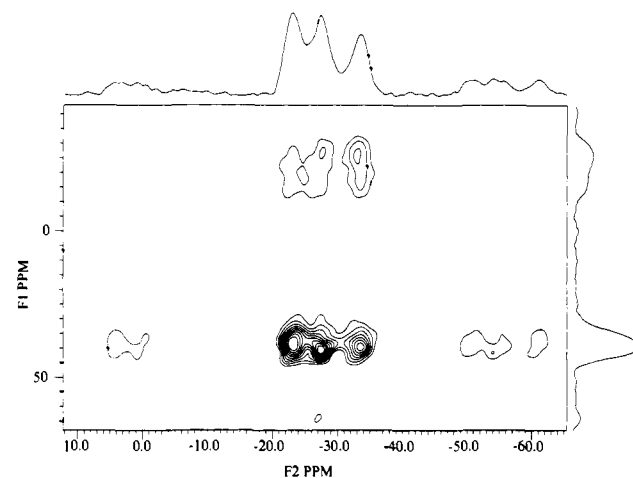


Figure 3. 2D-heteronuclear correlation spectrum of VPI-5. The F1 dimension was multiplied with a phased sine bell squared prior to Fourier transformation. The projection of the aluminum spectrum is displayed on the right of the 2D spectrum, the phosphorus spectrum at the top. For each subsequent experiment 10 000 scans were recorded, with a recycle delay of 0.25 s.

ppm to P1. The P2 and P3 sites have been assigned to, respectively, the  $^{31}\text{P}$  line at -23.7 and -27.5 ppm.<sup>13,14</sup>

The  $^{27}\text{Al}$ - $^{31}\text{P}$  double-resonance experiments were performed on a Bruker CXP-300 NMR spectrometer. The spinner speed was held constant at  $3332 \pm 1$  Hz. The magnetization was transferred from  $^{27}\text{Al}$  to  $^{31}\text{P}$  since the aluminum  $T_1$  is the shorter one. The  $^{31}\text{P}$  FID was measured after 15 rotor periods, of which 4 rotor periods were reserved for the REDOR pulse sequences. TPPI was applied to allow phase-sensitive detection in the F1 dimension.

Figure 3 displays the 2D spectrum of hydrated VPI-5. It shows that each phosphorus is connected with both tetrahedral aluminum and octahedral aluminum. However, the intensities of the cross-peaks differ. The three different phosphorus sites have a different surrounding of aluminum atoms: P1, 2Al1, Al2, Al3;

\* Present address: Physikalische Chemie FB6, Universität-GH-Duisburg, Lotharstrasse 1, 4100 Duisburg, Germany.

(1) Caravatti, P.; Brauschweiler, L.; Ernst, R. *Chem. Phys. Lett.* **1983**, *100*, 305.

(2) Franke, D.; Hudalla, C.; Eckert, H. *Solid State Nucl. Magn. Reson.* **1992**, *1* (1), 33-40.

(3) Hing, A. W.; Vega, S.; Schaefer, J. *J. Magn. Reson.* **1992**, *96*, 205-209.

(4) Gullion, T.; Schaefer, J. In *Advances in Magnetic Resonance*; Warren, W. S., Ed.; Academic Press: San Diego, CA, 1989; Vol. 13, pp 57-83.

(5) Davis, M. E.; Saldarriaga, C.; Montes, C.; Garces, J.; Crowder, C. *Nature* **1988**, *331*, 698-699.

(6) McCusker, L. B.; Baerlocher, Ch.; Jahn, E.; Bulow, M. *Zeolites* **1990**, *11*, 308-313.

(7) Wu, Y.; Chmelka, B. F.; Pines, A.; Davis, M. E.; Grobet, P. J.; Jacobs, P. A. *Nature* **1990**, *346*, 550-552.

(8) Grobet, P. J.; Samoson, A.; Geerts, H.; Martens, J. A.; Jacobs, P. A. *J. Phys. Chem.* **1991**, *95*, 9620-9622.

(9) Engelhardt, G., private communication.

(10) Davis, M. E.; Montes, C.; Hathaway, P. E.; Arhancet, J. P.; Hasha, D. L.; Garces, J. *J. Am. Chem. Soc.* **1989**, *111*, 3919-3924.

(11) Grobet, P. J.; Martens, J. A.; Balakrishnan, I.; Mertens, M.; Jacobs, P. A. *Appl. Catal.* **1989**, *56*, L21-L27.

(12) van Braam Houckgeest, J. P.; Kraushaar-Czarnetzki, B.; Dogterom, R. J.; de Groot, A. *J. Chem. Soc., Chem. Commun.* **1991**, 666-667.

(13) Perez, J. O.; Chu, P. J.; Clearfield, A. *J. Phys. Chem.* **1991**, *95*, 9994-9999.

(14) Kolodziejki, W.; He, H.; Klinowski, J. *Chem. Phys. Lett.* **1992**, *191* (1, 2), 117-124.

(15) Derouane, E. G.; Maistriau, L.; Gabelica, Z.; Tuel, A. B.; Nagy, J.; Ballmoos, R. *Appl. Catal.* **1989**, *51*, L13-L20.

(16) Maistriau, L.; Gabelica, Z.; Derouane, E. G.; Vogt, E. T. C.; van Oene, J. *Zeolites* **1991**, *11*, 583-592.

P2, A11, 2A12, A13, and P3, A11, A12, 2A13. P1 is the only phosphorus that is coordinated with two, instead of one, octahedral aluminum. Thus, the  $^{31}\text{P}$  peak at  $-33.6$  ppm must be assigned to P1.

Figure 3 also shows that the cross-peaks of the phosphorus lines at  $-23.3$  and  $-27.5$  ppm with the tetrahedral aluminum have different  $^{27}\text{Al}$  chemical shifts,  $38.3$  and  $40.3$  ppm, respectively. From  $^{27}\text{Al}$  DOR experiments,<sup>8</sup> it can be derived that the line at  $38.3$  ppm corresponds to the  $^{27}\text{Al}$  with the largest quadrupolar interaction. This is further substantiated by the larger line width in the F1 dimension. Bearing in mind that the P2 cross-peak with tetrahedral aluminum arises from the dipolar coupling to two A12 and one A13, and the P3 cross-peak from coupling to one A12 and two A13, we now have two possibilities. If the Grobet assignment for A12 and A13 is correct, then P2 resonates at  $-23.3$  ppm and P3 at  $-27.5$  ppm. This must be reversed when the Engelhardt assignment is correct. We conclude that this new type of 2D experiment is a useful tool for the correlation of NMR spectra.

**Acknowledgment.** We thank J. W. M. van Os and J. W. G. Janssen for technical assistance and Shell Amsterdam for the VPI-5 sample.

### Chiral N-Substituted Porphyrins Related to Heme Inactivation Products. First Crystallographic Determination of Absolute Stereochemistry and Correlation with Circular Dichroism

Katsuaki Konishi, Yoshinori Takahata, Takuzo Aida, and Shohei Inoue\*

Department of Synthetic Chemistry, Faculty of Engineering  
University of Tokyo, Hongo, Bunkyo-ku, Tokyo 113 Japan

Reiko Kuroda†

College of Liberal Arts and Sciences, University of Tokyo  
Komaba, Meguro-ku, Tokyo 153 Japan

Received October 8, 1992

There are various naturally occurring and artificial porphyrins with enantiotopic faces (prochiral) due to specific arrangements of the peripheral substituents, and they can be converted into chiral porphyrins.<sup>1-4</sup> From a biological viewpoint, chiral N-substituted porphyrins with asymmetric nitrogen atoms are the most attractive.<sup>5</sup> Ortiz de Montellano et al. have demonstrated that iron protoporphyrin IX is denatured into the N-substituted derivatives during the metabolic processes mediated by hemoproteins.<sup>6</sup> Since protoporphyrin IX has enantiotopic faces, the N-substituted derivatives are chiral. In fact, some optically active N-substituted protoporphyrins IX have been isolated from metabolic systems.<sup>7</sup> However, to date, there are no chiral N-substituted porphyrins whose absolute structures have been defined by X-ray crystal-

\* Responsible for the X-ray crystallography in this work.

(1) For chiral N-substituted porphyrins: Kubo, H.; Aida, T.; Inoue, S.; Okamoto, Y. *J. Chem. Soc., Chem. Commun.* **1988**, 1015.

(2) For chiral alkyl- and arylcobalt(III) porphyrins: Konishi, K.; Sugino, T.; Aida, T.; Inoue, S. *J. Am. Chem. Soc.* **1991**, *113*, 6487.

(3) For chiral meso-substituted porphyrins: Konishi, K.; Miyazaki, K.; Aida, T.; Inoue, S. *J. Am. Chem. Soc.* **1990**, *112*, 5639.

(4) For chiral strapped porphyrins: Konishi, K.; Oda, K.; Nishida, K.; Aida, T.; Inoue, S. *J. Am. Chem. Soc.* **1992**, *114*, 1313. Chiang, L.-c.; Konishi, K.; Aida, T.; Inoue, S. *J. Chem. Soc., Chem. Commun.* **1992**, 254.

(5) Lavalley, D. K. *The Chemistry and Biochemistry of N-Substituted Porphyrins*; VCH: New York, 1987.

(6) (a) Ortiz de Montellano, P. R. *Annu. Rep. Med. Chem.* **1984**, *19*, 201.

(b) Ortiz de Montellano, P. R.; Correia, M. A. *Annu. Rev. Pharmacol. Toxicol.* **1983**, *23*, 481.

(7) (a) Ortiz de Montellano, P. R.; Kunze, K. L.; Beilan, H. S. *J. Biol. Chem.* **1983**, *258*, 45. (b) Kunze, K. L.; Mangold, B. L. K.; Wheeler, C.; Beilan, H. S.; Ortiz de Montellano, P. R. *J. Biol. Chem.* **1983**, *258*, 4202. (c) Ortiz de Montellano, P. R.; Mangold, B. L. K.; Wheeler, C.; Kunze, K. L.; Reich, N. O. *J. Biol. Chem.* **1983**, *258*, 4208. (d) Augusto, O.; Kunze, K. L.; Ortiz de Montellano, P. R. *J. Biol. Chem.* **1982**, *257*, 6231. (e) Ortiz de Montellano, P. R.; Kunze, K. L. *Biochemistry* **1981**, *20*, 7266. (f) Swanson, B. A.; Ortiz de Montellano, P. R. *J. Am. Chem. Soc.* **1991**, *113*, 8146.

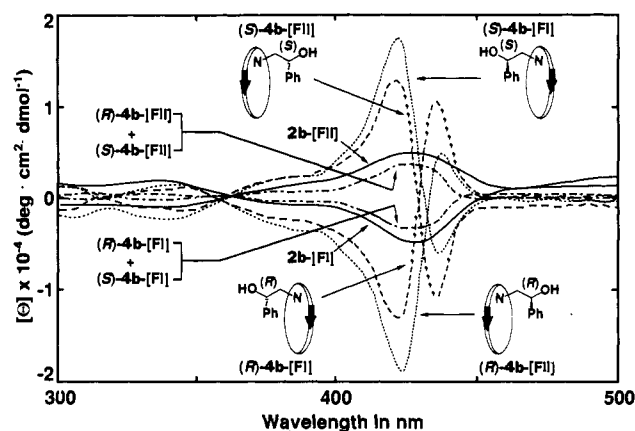
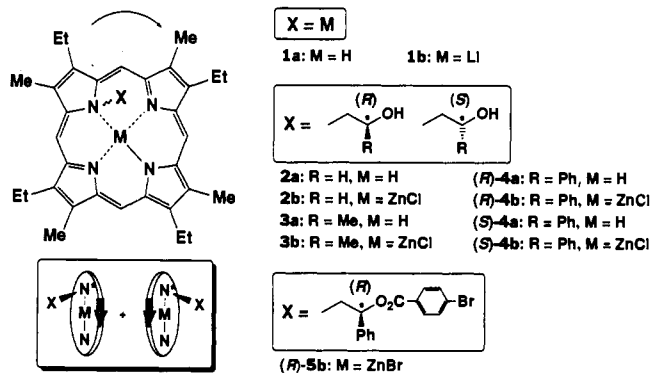


Figure 1. Circular dichroism spectra ( $\text{CHCl}_3$ ,  $4.3 \times 10^{-5}$  M) of the chloro zinc complexes of the isomers of chiral *N*-(2-hydroxyethyl)etioporphyrin I (**2b**) and *N*-[2-hydroxy-2-phenylethyl]etioporphyrin I (**4b**). The arrows in the schematic illustrations of the isomers indicate the Me  $\rightarrow$  Et sequence in each pyrrole unit.

lography. The present communication describes the first crystallographic determination of the absolute configuration of a chiral *N*-(2-hydroxyalkyl)etioporphyrin I derivative (**5b**), related to the products of the inactivation of cytochrome P-450 with olefins,<sup>8</sup> and provides a clear correlation with circular dichroism.



For the synthesis of a series of *N*-(2-hydroxyalkyl)etioporphyrins I,<sup>9</sup> a novel, efficient route was used, which involves nucleophilic ring opening of epoxides with lithiated etioporphyrin I (**1b**).<sup>10</sup> For example, the reaction of **1b** with ethylene oxide followed by metalation afforded the chloro zinc complex of *N*-(2-hydroxyethyl)etioporphyrin I (**2b**)<sup>11</sup> in 96% yield. When monosubstituted epoxides such as propylene oxide and styrene oxide were reacted with **1b**, they were cleaved exclusively at the O-CH<sub>2</sub> bonds with retention of configuration, to give **3b** and **4b**, respectively, in 78 and 76% yields.<sup>11</sup> In all these cases, no *N,N'*-disubstituted porphyrins were formed.

Due to the enantiotopic structure of etioporphyrin I (**1a**), **2** should be racemic, while **3** and **4** should be mixtures of diastereoisomers. The isomers of **2a-4a** in the free-base forms<sup>11</sup> were resolved by chiral HPLC.<sup>1</sup> For example, racemic **2a** showed two elution peaks with comparable peak areas (fraction I, **2a**-[FI]; fraction II, **2a**-[FII]). On the other hand, for diastereoisomeric *N*-[(*R*)-2-hydroxy-2-phenylethyl]etioporphyrin I (*(R)*-**4a**) derived

(8) Ortiz de Montellano, P. R.; Beilan, H. S.; Kunze, K. L.; Mico, B. A. *J. Biol. Chem.* **1981**, *256*, 4395.

(9) One-pot electrophilic N-substitution with alkyl iodides (Cavaleiro, J. A. S.; Condoso, M. F. P. N.; Jackson, A. H.; Neves, M. G. P. M. S.; Rao, K. R. N.; Sadasiva, B. K. *Tetrahedron Lett.* **1984**, *25*, 6047) gave *N*-(hydroxyalkyl)porphyrins in very low yields. Another method utilizing cobalt porphyrins (Setsune, J.; Dolphin, D. *J. Org. Chem.* **1985**, *50*, 2958) involves a multistep redox process and is not convenient for large-scale synthesis.

(10) For dilithium salts of porphyrins: (a) Arnold, J. J. *Chem. Soc., Chem. Commun.* **1990**, 976. (b) Buchler, J. W.; De Cian, A.; Fischer, J.; Hamerschmitt, P.; Weiss, R. *Chem. Ber.* **1991**, *124*, 1051.

(11) All these compounds were unambiguously identified by  $^1\text{H}$  NMR or FAB-HRMS, and characterized by UV-visible spectroscopy.